

Panel Presentation Session: IN SITU TESTING TECHNIQUES
XI INTERNATIONAL CONFERENCE ON SOIL MECHANICS AND
FOUNDATION ENGINEERING
San Francisco - USA 1985

Vol. 5, pp.
2667-2673

SYNOPSIS Existing methods of field determination of K_0 in sand are subdivided into direct, semidirect, indirect methods. One particular indirect method (Schmertmann, 1983) is discussed in detail, based on the parallel measurement and interpretation of matching pairs of K_0 from DMT and q_c from CPT. A compact K_0 -chart is worked out using this method, permitting to read directly K_0 from K_D and q_c . Sensitivity diagrams are shown illustrating the different sensitivity of K_D and q_c to K_0 and ϕ . Additional calibration information, in the form of an additional scale, is added in the K_0 chart, summarizing the results of recent extensive CPT-DMT investigations in the Po river sand.

1 INTRODUCTION

The determination of the coefficient of earth pressure at rest K_0 in sand is probably one of the most difficult tasks of in situ testing. The action of the measurement itself alters what is being measured.

In a recent paper in the Prof. Osterberg Volume, Schmertmann (1985) lists 17 methods of K_0 determination. However most of them are for clays, while only few are applicable to sands.

The laboratory methods suffer from the well known difficulty of recovering samples of adequate quality and are generally considered inadequate for predicting K_0 in sand.

At present, only field methods are believed to have the potential for such determination, despite their inherent disadvantage of requiring the insertion of some type of instrument.

2 CLASSES OF FIELD METHODS

From the methodological point of view, the field methods for the determination of K_0 may be subdivided into 3 classes:

- Direct methods
- Semidirect or back extrapolation methods
- Indirect methods

2.1 Direct Methods

Direct methods try to measure K_0 directly, by attempting insertion with zero disturbance. The only existing instrument able in principle to measure directly K_0 is the Self Boring Pressure meter. Some researchers, however, question this possibility even in principle. E.g. Fahey and Randolph (1985) argue that, in sand, even the penetration of an infinitely thin hollow cylinder would produce significant stress alteration. Because of interlocking of sand grains, some movement of the grains still has to occur to allow passage of the cylinder. According to Fahey and Randolph such movement is sufficient to alter substantially K_0 . The question has conceptual value, because by technology we cannot hope to outperform the infinitely thin hollow cylinder.

2.2 Semidirect or Back Extrapolation Methods

This designation is reserved herein to methods which, by back extrapolation, try to figure what the response would have been in absence of instrument. These methods still have a "direct" philosophy because, if the extrapolation is successful, then K_0 can be determined separately from other parameters. An instrument well exemplifying this class is the Handy stepped blade (Handy et al. 1982). The principle of this instrument is to measure the lateral stress against sections of the blade of different thickness and to back extrapolate the lateral stress to zero thickness. Such extrapolation, however, is not free from problems. In particular

- A blade of zero thickness does not mean no blade, because it still causes movement of the grains, as discussed for the SBPM.
- The lateral pressure does not always increase with blade thickness, as presupposed by the method.
- Even thin blades may bring soil conditions far from the origin, and back extrapolation may not work (Fig. 1).

2.3 Indirect Methods

Other in situ penetration tests (SPT, CPT, DMT) bring the soil even further up in the stress-strain curve (Fig. 1), thus calling into play the entire stress-strain-strength behaviour of the soil. The direct determination of an isolated parameter independently from others is no longer possible. The rigorous interpretation becomes a formidable task, as it requires the complete theoretical solution of the penetration problem and a soil modeling involving soil properties yet to be determined. One simplified way of attacking the problem may involve the following steps:

- To pursue the determination of a few simple (or simplified) parameters, such as "modulus", "friction angle", K_0 .
- To measure in situ a number of independent soil responses, possibly each one dominated by one of the simplified parameters.
- To infer from such responses the unknown parameter

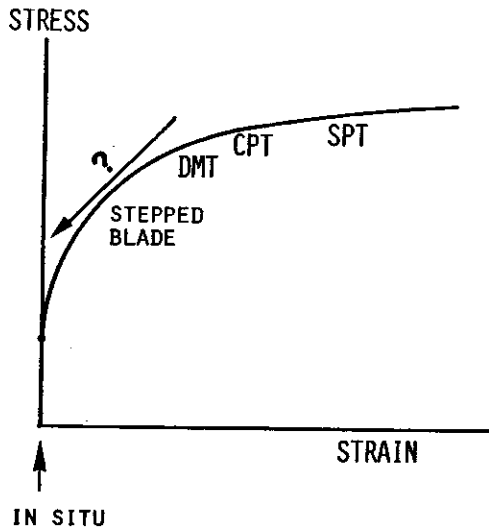


Fig.1 Schematic Diagram Illustrating Qualitatively Insertion Effects.

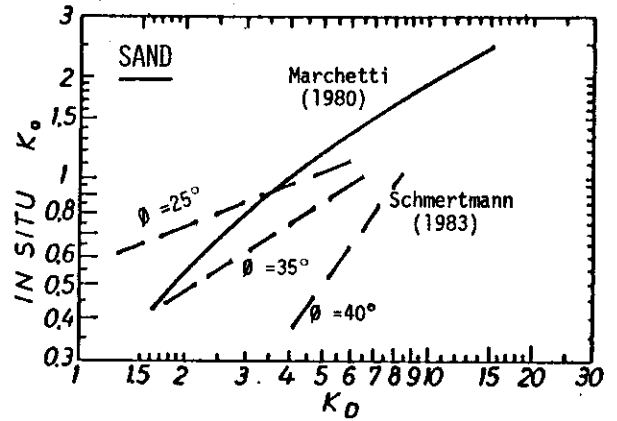


Fig.2 Correlations K_0 vs K_D
 -Solid curve : Initial 1980 Correlation
 -Dashed curves : Schmertmann's 1983 correlations (re-plotted).

meters.

On the other hand factors such as the shape of the stress strain curve, volumetric strain properties, unloading behaviour etc. may have considerable influence on the penetration response. Thus, only approximate correlations can, at best, be obtained in this way.

The rest of this contribution will deal with one particular method of K_0 determination, based on DMT plus CPT results, developed by Schmertmann in 1983, on which the writer had some first hand experience. Hereunder, reference will always be to the following conditions:

- DMT advanced quasi-statically (jacked)
- CPT performed with electrical cone
- Clean sand (drained conditions)

3 THE DMT & CPT METHOD

3.1 The Initial (1980) K_0 vs K_D Correlation

When the dilatometer blade penetrates into sand, it causes lateral displacement and, in general, an increase of the pre-existing horizontal stress σ_h to a higher value p_0 , measured by DMT. In non dimensional terms, the pre-insertion K_0 is increased to K_D . E.g. in a NC sand, where $K_0=0.4-0.5$, typically $K_D \approx 2$ to 4 (some 5 times higher). Early in the development of DMT it was noted that, in OC soils, where K_0 is higher, even K_D was higher. Hence the correlation K_0 vs K_D was investigated. The solid line in Fig.2 shows the correlation based on the data points available in 1980 (Marchetti, 1980). However most of these data points were for clays and only two for sands. Thus, in sands, the then available data were insufficient to draw any conclusion. Later data referring to sands, obtained from calibration chamber (CC) tests, clearly indicated the necessity, for sands, of introducing in the correlations K_0 vs K_D the relative density D_r (or ϕ) as a parameter, as D_r played a major role in the correlation.

3.2 The Schmertmann K_0 - K_D - ϕ Correlation (1983)

Based on the CC data available up to 1983, Schmertmann draw tentative correlations K_0 vs K_D with ϕ as a parameter, which are superimposed in Fig.2 to the initial 1980 correlation (it may be noted that the 1980 correlation corresponds, according to the 1983 correlations, to loose sands). Such K_0 - K_D - ϕ correlation was expressed analytically by Schmertmann as follows:

$$K_0 = \frac{40+23 \cdot K_D - 86 \cdot K_D (1 - \sin \phi_{ax}) + 152 (1 - \sin \phi_{ax}) - 717 (1 - \sin \phi_{ax})^2}{192 - 717 (1 - \sin \phi_{ax})} \quad (1)$$

where ϕ_{ax} is the angle of shearing resistance as determined by standard triaxial compression tests (same as ϕ herein).

3.3 The Schmertmann's Durgunoglu and Mitchell Method (1983)

Eq.1, to be used, requires the knowledge of ϕ , usually unknown too. Therefore Schmertmann suggested to measure simultaneously K_D from DMT and q_c from CPT (or q_D , the dilatometer tip resistance), from which both the unknowns K_0 and ϕ could be simultaneously determined. For such determination Schmertmann suggested to combine Eq.1 with the Durgunoglu and Mitchell (D&M) theory (1975), also expressing q_c as a function of the two unknowns K_0 and ϕ . Thus he obtained the following system of two equations in the two unknowns K_0 and ϕ :

$$\begin{cases} K_D = f_1(K_0, \phi) & \text{(Eq.1 above, solved for } K_D) \\ q_c = f_2(K_0, \phi) & \text{(D\&M theory)} \end{cases} \quad (2)$$

The system 2 can be solved by an iterative procedure described in detail by Schmertmann (1983). Here it is only noted that the D&M equations are mathematically complex so that the iterative procedure is generally performed by computer.

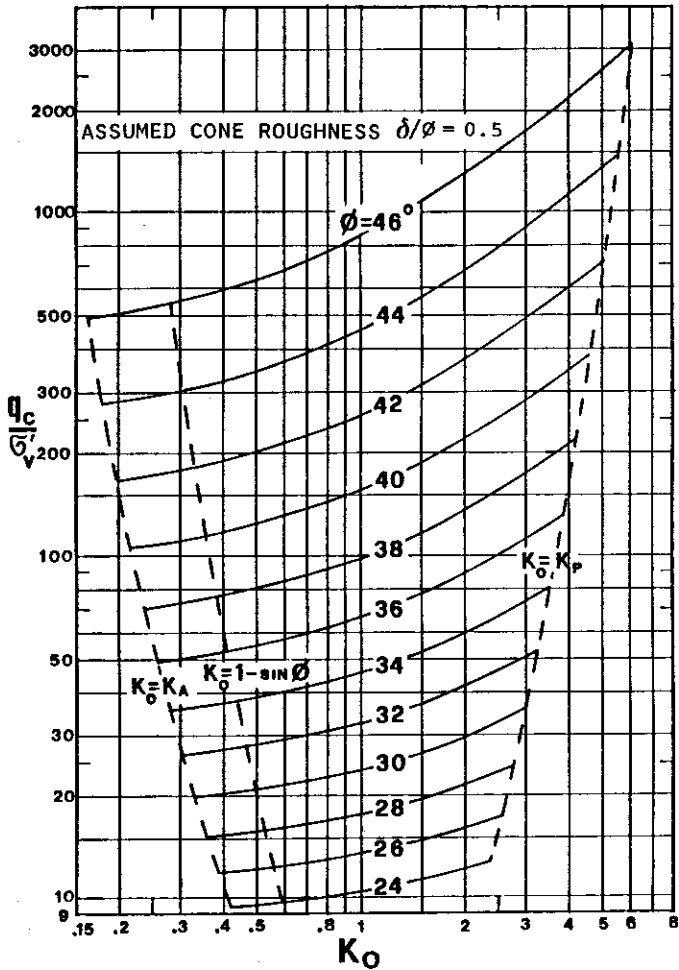


Fig. 3 Chart for Interpreting ϕ from CPT requiring an evaluation of K_o (worked out by the writer from the Durgunoglu and Mitchell 1975 Equations).

3.4 Compact Graphical Form of the D&M Equations

The D&M equations, used in the Schmertmann's method, have been summarized by the writer in the chart in Fig. 3. This chart permits to estimate ϕ from q_c if an evaluation of K_o is also available.

(The D&M theory predicts, except at very shallow depths, a linear increase of q_c with depth, for given values of K_o and ϕ . Thus, except at very shallow depths, q_c can be normalized to q_{c30} , there by eliminating one variable. An analysis of the chart error at shallow depths has shown:

- for $z=2m$, the maximum difference between $\phi_{D\&M}$ and ϕ predicted by the chart is 0.2 degrees
- for $z=1m$ the maximum error is 0.8 degrees

These errors are found in the most unfavourable zone in the chart, i.e. for $\phi=46^\circ$ and $K=K_P$. For less extreme values of ϕ and K_o the error is much smaller and, even for $z=1m$, less than the chart reading error).

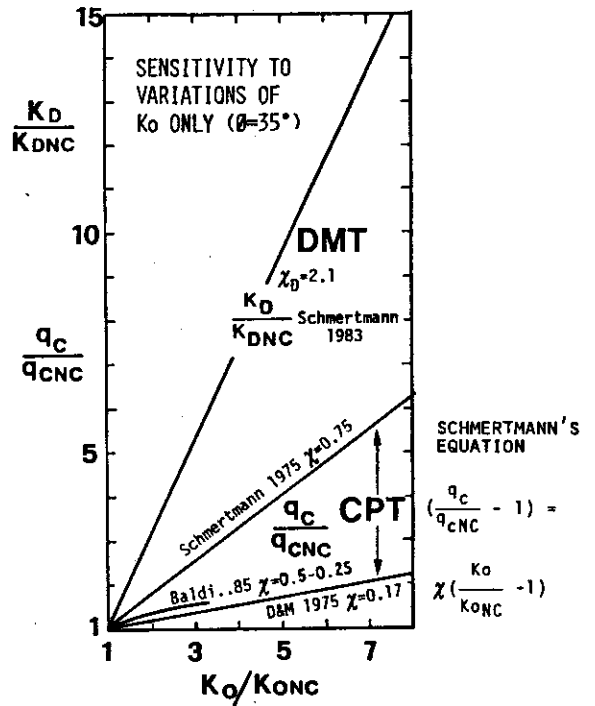


Fig. 4 Normalized Sensitivity to K_o of K_D and q_c .

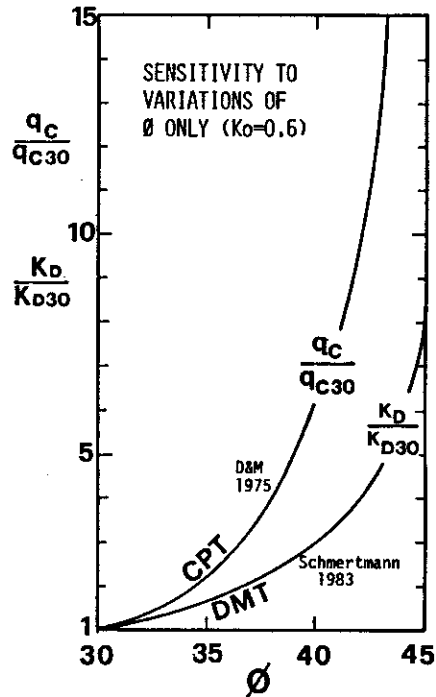


Fig. 5 Normalized Sensitivity to ϕ of q_c and K_D .

3.5 Sensitivity of K_D and q_c to K_O and ϕ

For a better understanding of the Schmertmann D&M method, it is instructive to examine the different sensitivity of K_D and q_c to the two unknown variables K_O and ϕ .

The sensitivity graph in Fig. 4 shows how q_c and K_D react to changes of K_O alone. Both axes display variables normalized to their NC value. In all cases it has been assumed $\phi = \text{const} = 35^\circ$. Despite some differences in χ according to various authors, Fig. 4 clearly shows that K_D is several times more responsive than q_c to changes of K_O .

The sensitivity graph in Fig. 5 shows how q_c and K_D react to changes of ϕ alone. In the vertical axis q_c and K_D have been normalized to their values for $\phi = 30^\circ$. In all cases it has been assumed $K_O = \text{const} = 0.6$. Fig. 5 shows that q_c is considerably more responsive than K_D to changes in ϕ . In conclusion both q_c and K_D depend on both K_O and ϕ , but q_c reflects more ϕ , K_D reflects more K_O .

3.6 The Compact K_O Chart

As noted earlier, the Schmertmann's D&M method requires complex computations, generally performed by computer. For quick and direct applications the writer has found useful to draw the chart in Fig. 6, obtained using the Schmertmann's D&M method. The only unknown in the chart is K_O , having eliminated the other unknown ϕ . The K_O chart in Fig. 6 permits to read directly K_O from K_D and q_c . Once K_O has been estimated, then ϕ can be read from the chart in Fig. 3.

The chart in Fig. 6 may be used readily by engineers unfamiliar with the complex computer programs otherwise needed. The chart may also be helpful for parametric studies and for identifying trends. E.g. it permits to note that some uncertainty in q_c is tolerable without a significant loss of definition in determining K_O . Even more importantly, Fig. 6 provides an interesting alternative format in which the data points may be drawn. In fact:

- The chart expresses K_O as a function of 2 highly reproducible measurements (K_D and q_c), bypassing the intermediate determination of ϕ (or worse D_r), representing an unneeded potential source of ambiguity.
- The combined use of the Schmertmann K_O - K_D - ϕ correlation plus the D&M theory brings in the inevitable approximations inherent in both, which are probably corrected most efficiently by plotting the experimental results in the format of Fig. 6, having, at least partially, a theoretical origin.

It should be noted that, in Fig. 6, the $q_c/\sigma'_v = \text{constant}$ curves are not curves of constant ϕ (or D_r), because the D&M equations by which q_c is calculated, already account for the dependence of q_c/σ'_v from K_O , besides ϕ . When sufficient data will justify refinements, it will be worth verifying if the use of $q_c/\sigma'_v{}^m$ (with the exponent m between 0.6 and 0.8) rather than q_c/σ'_v , may lead to better correlations. It is noted that there are many alternative forms in which Fig. 6 may be drawn, e.g. K_D vs q_c/σ'_v with K_O as a parameter on the curves, K_O vs K_D with the ratio q_c/p_o as a parameter ($p_o = \text{first corrected DMT reading}$) etc.

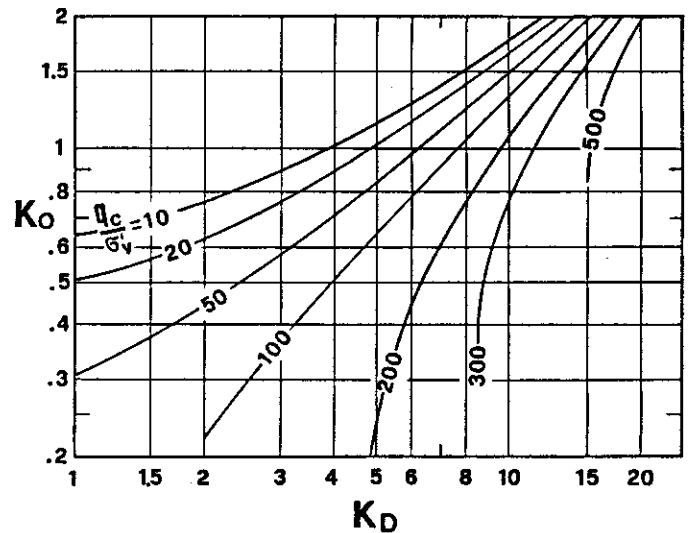


Fig. 6 Chart for interpreting K_O from K_D (DMT) and q_c (CPT) worked out by the writer using the Schmertmann's Durgunoglu and Mitchell procedure.

3.7 The K_O Chart vs the Po River Sand Data

An opportunity of evaluating the chart in Fig. 6 was offered to the writer by the availability of some 90 pairs of parallel close DMT and CPT (electrical) soundings, in the Po river valley sand. This sand is a recently sedimented, geologically normally consolidated, slightly overconsolidated sand, with the preconsolidation mechanism due to aging and GWL oscillations, with an evaluated OCR ranging from 1.3 to 1.7 and an evaluated K_O ranging from 0.5 to 0.6 (Jamiołkowski et al., Section 3.2.4, 1985).

From the large mass of available data, the writer selected 25 pairs of values of matching q_c and K_D . During the selection the overriding concern was to pick up values from well characterized and definitely corresponding layers (this concern would have been avoided if a multiple sensor probe was available). These pairs of q_c and K_D are listed, with additional information, in Table I and are plotted in Fig. 7.

From q_c and K_D values of K_O have been interpreted, using the Schmertmann's D&M procedure (or Fig. 6). These values are also listed in Table I and plotted in Fig. 7 (C). It is noted:

- 1 The average of the predicted K_O is 0.92, considerably higher than the estimated 0.55.
- 2 The coefficient of variation of K_O ($\sim 30\%$) is attenuated compared with the coefficient of variation of K_D ($\sim 41\%$). This is because, at this site, high K_D are generally accompanied by high q_c/σ'_v , so that, in the Schmertmann's D&M interpretation, part of the responsibility of the high K_D is attributed to a high ϕ , and not entirely to K_O .

TABLE I

Results of Parallel CPTs and DMTs in the Po River Valley Sand

#	TEST	Z _i (m)	Z _f (m)	Z _{ave} (m)	σ' _v (bar)	K _D	I _D	E _D (bar)	q _c (bar)	f _s	q _c /σ' _v	β _{SDM}	K _o SDM	K _o '
1	4031	5.5	6.5	6.0	.52	6.0	2.5	300	60	.30	115	39.24	.73	.33
2	5025	6.0	7.0	6.5	.58	9.0	2.3	420	95	.45	164	40.22	1.02	?
3	4047	8.0	12.0	10.0	.91	6.5	1.8	350	100	.50	110	38.81	.82	.53
4	5041	10.2	10.2	10.2	.80	5.0	2.7	400	75	.25	94	38.38	.67	.44
5	4010	10.0	12.0	11.0	1.00	7.5	2.1	550	105	.50	105	38.35	.97	.70
6	4027	10.0	12.0	11.0	1.00	12.0	1.8	800	150	1.20	150	39.16	1.46	.84
7	5009	11.5	12.5	12.0	1.02	6.0	2.2	450	110	.50	108	38.87	.76	.50
8	4031	11.5	12.5	12.0	1.10	8.0	2.1	650	130	.60	118	38.81	1.00	.64
9	4005	12.0	14.0	13.0	1.22	7.0	1.7	500	130	.80	107	38.52	.90	.64
10	5014	12.0	14.0	13.0	1.06	10.3	1.6	680	145	1.00	137	39.04	1.27	.74
11	5038	12.0	14.0	13.0	1.05	11.0	1.4	650	160	1.10	152	39.42	1.33	.70
12	5033	12.0	17.0	14.5	1.20	8.0	1.6	650	150	.85	125	38.93	1.09	.70
13	4027	15.8	15.8	15.8	1.45	12.0	1.6	1000	250	4.00	172	39.79	1.42	?
14	5009	15.5	16.5	16.0	1.42	6.0	1.9	550	140	.80	99	38.38	.79	.54
15	5041	15.0	18.0	16.5	1.33	6.0	2.6	600	170	.90	120	39.73	.70	?
16	4002	18.0	18.0	18.0	1.82	12.0	1.4	1015	300	2.30	165	39.59	1.43	.70
17	4002	17.0	19.0	18.0	1.82	10.0	1.7	1050	270	2.05	140	39.50	1.20	.48
18	5009	19.5	20.5	20.0	1.86	5.5	1.9	680	140	1.00	75	37.05	.80	.68
19	5038	18.0	22.0	20.0	1.79	5.0	1.5	480	120	.90	67	36.53	.76	.67
20	5040	20.0	24.0	22.0	2.04	4.7	1.7	600	110	1.00	54	35.35	.78	.70
21	4010	21.0	25.0	23.0	2.23	4.5	1.6	500	150	.80	67	36.68	.70	.60
22	4022	20.0	26.0	23.0	2.12	4.5	1.6	620	140	1.20	66	36.56	.70	.68
23	4002	22.0	26.0	24.0	2.53	3.0	1.8	500	140	1.00	55	35.96	.55	.48
24	5003	25.0	29.0	27.0	2.63	2.6	2.0	500	115	1.15	44	34.63	.55	.50
25	5036	32.0	34.0	33.0	3.00	2.6	2.0	500	115	.75	38	33.80	.58	.52
Average 0.92 0.60														

Legend

- Z_i, Z_f, Z_{ave} = initial, final, average depth of layer
- σ'_v = vertical effective overburden stress
- K_D, I_D, E_D = intermediate DMT parameters
- q_c, f_s = CPT tip resistance and sleeve friction
- K_o, SDM and β_{SDM} = K_o and β derived from K_D and q_c using the Schmertmann D&M procedure (or Figs.6 and 3)
- K_o' = value of K_o derived from K_D and q_c using Fig.9 with modified scale

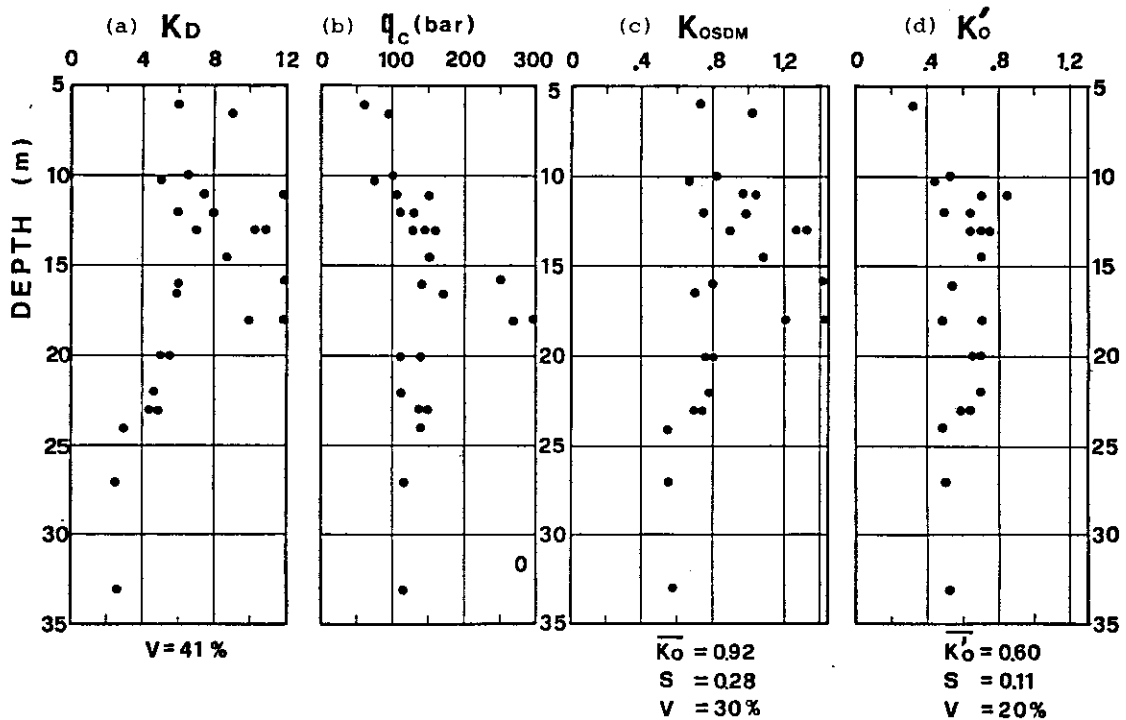


Fig.7 Results of parallel DMTs and CPTs in the Po River Valley Sand

- (a) and (b) : Pairs of values of K_D and q_c in corresponding layers
- (c) : K_o derived from K_D and q_c using the Schmertmann D&M procedure (or Fig.6)
- (d) : K_o derived from K_D and q_c using Fig.9 with modified scale

\bar{X} = average of X S = Standard Deviation V = Coefficient of variation = S/ \bar{X}

3 Despite this attenuation, the variation in the interpreted K_0 is still considerable. An important question requiring clarification is if such variation reflects:

- a Actual variations of K_0 in the ground
- b Local prestressing (at least in the loosest layers, where prestressing increases K_D and hence the interpreted K_0)
- c Local cementation (but no evidence of cementation was noted so far in this intensely investigated site)
- d Other effects

4 The data listed in Table I carry a heavy experimental weight for several reasons:

- a They are representative of a much larger mass of accurately taken field measurements
- b They have been collected in the field, so they are certainly free from boundary conditions uncertainties, as it is the case with calibration chamber data, especially at high D_r
- c If it is accepted that the in situ value of K_0 in this deposit is nearly 0.55 (and indeed it is difficult to find reasons why K_0 should be appreciably outside the range 0.50 to 0.60), then the 25 data points in Table I are equivalent to 25 CC data points

3.8 The Dual Scale K_0 Chart

In view of the above, it is possible that the field data may reflect reality more than the CC data on which Fig. 6 is based. It was therefore considered of interest to investigate how Fig. 6 would modify if it had to accommodate the Po river data. To do this, it was assumed for the deposit the field value $K_0=0.55$. The horizontal line $K_0=0.55$ was drawn in Fig. 6. The intersection of this line with the curves in Fig. 6 define the correspondence existing, according to Fig. 6, between q_c/σ'_v and K_D for $K_0=0.55$ (dashed line in Fig. 8). However the Po river data define such correspondence too (solid line in Fig. 8). The difference is considerable, especially for the denser (high q_c/σ'_v) layers. A simple way of modifying Fig. 6 for a better agreement with the Po data is to assume that the shape of the curves in Fig. 6 is correct, but the q_c/σ'_v values for each curve are those prescribed by the solid line in Fig. 8. By so doing, an additional scale for q_c/σ'_v is obtained, as shown in Fig. 9.

In all, the Po river data suggest a shift of the curves towards the right, especially for high K_D values (i.e. in the zone where items 3b and 4b in section 3.7 suggest that the field data may be more representative than the CC data).

Fig. 7d shows K_0' values that one would obtain from the pairs of K_D and q_c using the modified scale in Fig. 9. It is noteworthy that not only has the average K_0 decreased from 0.92 to 0.60 (expectable) but also the coefficient of variation has decreased appreciably, from 30% to 20%, lending some support to the modified scale.

In conclusion the K_0 chart in Fig. 9, with its dual scale, summarizes all the experimental information available so far - to the writer - and is the one he would use today to evaluate K_0 from K_D and q_c . On the other hand it should be emphasized that Fig. 9 still requires considerable CC and field verification.

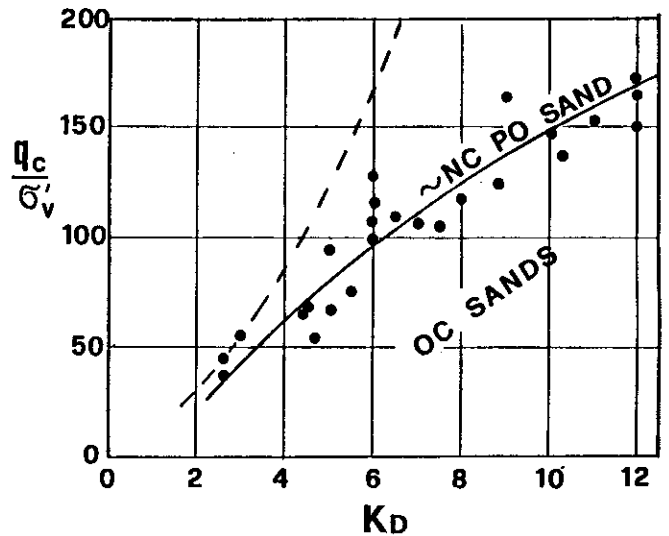


Fig. 8 Relationship q_c/σ'_v vs K_D for :
 Solid line : nearly NC Po River Sand (OCR 1.5)-least square parabola
 Dashed line: as predicted from Fig. 6 for $K_0=0.55$

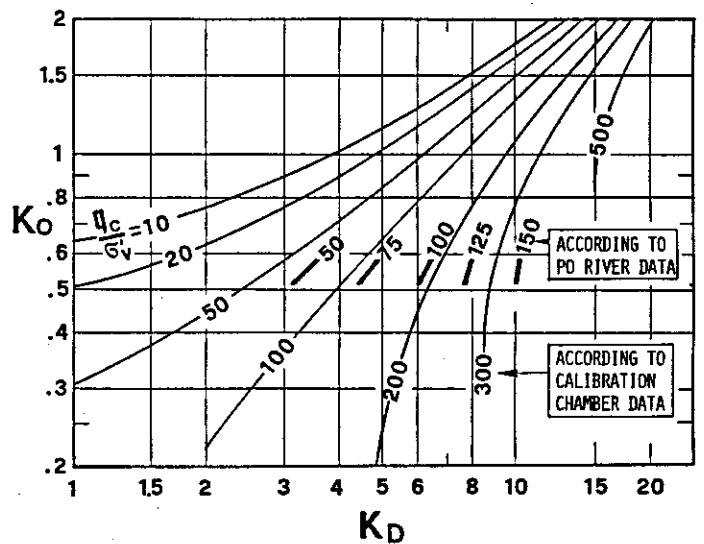


Fig. 9 Chart for Interpreting K_0 from K_D (DMT) and q_c (CPT), with a dual scale :
 (1) According to Calibration Chamber data
 (2) According to Po River Field data.

REFERENCES

- Baldi, G., Bellotti, R., Ghionna, V., Jamiolkowski, M., Pasqualini, E. (1985). Penetration Resistance and Liquefaction of Sands. Proc. of the XI ICSMFE, San Francisco.
- Durgunoglu, H.T. and Mitchell, J.K. (1975). Static Penetration Resistance of Soils, I-Analysis, II-Evaluation of Theory and Implications for Practice, ASCE Spec. Conf. on In Situ Measurement of Soil Properties, Raleigh NC, Vol. I, pp. 151-189.
- Fahey, M. and Randolph, M.F. (1985). Discussion of "Effect of Disturbance on Parameters Derived from Self-Boring Pressuremeter Tests in Sand", Géotechnique 35, No. 2, pp. 221-222.
- Handy, R.L., Remmes, B., Moldt, S., Lutenecker, A.J., Trott, G. (1982). In Situ Stress Determination by Iowa Stepped Blade. ASCE Jnl GED, GT11, pp. 1405-1422.
- Jamiolkowski, M., Ladd, C.C., Germaine, J.T. and Lancellotta, R. (1985). New Developments in Field and Laboratory Testing of Soils. SOA Report, XI ICSMFE, San Francisco, Aug. 1985.
- Marchetti, S. (1980). In Situ Tests by Flat Dilatometer. ASCE Jnl GED, GT3, pp. 299-321.
- Schmertmann, J.H. (1983). Revised Procedure for Calculating K_0 and OCR from DMT's with $I_p > 1.2$ and which incorporate the Penetration Force Measurement to permit Calculating the Plain Strain Friction Angle. DMT Workshop 16-18 March, Gainesville, Florida.
- Schmertmann, J.H. (1985). Measure and Use In Situ Lateral Stress. Osterberg Volume, Northwestern University, Dept. of Civil Engineering, pp. 189-213.